

# Product Datasheet

## HSPA8/HSC71/Hsc70 Antibody (13D3) NB120-2788

Unit Size: 100 ul

Store at -20C. Avoid freeze-thaw cycles.

[www.novusbio.com](http://www.novusbio.com)



[technical@novusbio.com](mailto:technical@novusbio.com)

**Reviews: 2 Publications: 32**

Protocols, Publications, Related Products, Reviews, Research Tools and Images at:  
[www.novusbio.com/NB120-2788](http://www.novusbio.com/NB120-2788)

Updated 9/9/2025 v.20.1

**Earn rewards for product  
reviews and publications.**

Submit a publication at [www.novusbio.com/publications](http://www.novusbio.com/publications)

Submit a review at [www.novusbio.com/reviews/destination/NB120-2788](http://www.novusbio.com/reviews/destination/NB120-2788)



**NB120-2788****HSPA8/HSC71/Hsc70 Antibody (13D3)**

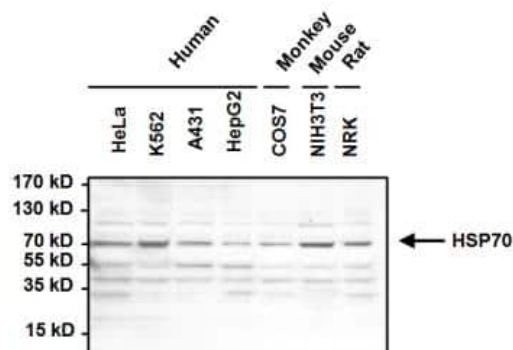
<b>Product Information</b>	
<b>Unit Size</b>	100 ul
<b>Concentration</b>	This product is unpurified. The exact concentration of antibody is not quantifiable.
<b>Storage</b>	Store at -20C. Avoid freeze-thaw cycles.
<b>Clonality</b>	Monoclonal
<b>Clone</b>	13D3
<b>Preservative</b>	0.05% Sodium Azide
<b>Isotype</b>	IgM
<b>Purity</b>	Unpurified
<b>Buffer</b>	Ascites diluted with PBS
<b>Target Molecular Weight</b>	70 kDa
<b>Product Description</b>	
<b>Description</b>	Novus Biologicals Mouse HSPA8/HSC71/Hsc70 Antibody (13D3) (NB120-2788) is a monoclonal antibody validated for use in IHC, WB, Flow, ICC/IF, Simple Western and IP. Anti-HSPA8/HSC71/Hsc70 Antibody: Cited in 30 publications. All Novus Biologicals antibodies are covered by our 100% guarantee.
<b>Host</b>	Mouse
<b>Gene ID</b>	3312
<b>Gene Symbol</b>	HSPA8
<b>Species</b>	Human, Mouse, Rat, Bovine, Feline, Fish, Hamster, Primate
<b>Reactivity Notes</b>	Reported cross-reactivity with Bovine in literature (Terlecky et al.). Hamster reactivity reported in scientific literature (PMID: 16737757). Fish reactivity reported in scientific literature (PMID: 9006893). Rat reactivity reported by customer review. Please note that this antibody is reactive to Mouse and derived from the same host, Mouse. Additional Mouse on Mouse blocking steps may be required for IHC and ICC experiments. Please contact Technical Support for more information.
<b>Specificity/Sensitivity</b>	This displays slight cross-reactivity to HSP 70.
<b>Immunogen</b>	Mouse spermatogenic cell protein.
<b>Product Application Details</b>	
<b>Applications</b>	Western Blot, Simple Western, Immunohistochemistry-Paraffin, Flow Cytometry, Immunoblotting, Immunocytochemistry/ Immunofluorescence, Immunohistochemistry, Immunohistochemistry-Frozen, Immunoprecipitation, Block/Neutralize
<b>Recommended Dilutions</b>	Western Blot 1:1000 - 1:5000, Simple Western 1:2000, Flow Cytometry 1:10 - 1:1000, Immunohistochemistry 1:20 - 1:200, Immunocytochemistry/ Immunofluorescence 1:20 - 1:200, Immunoprecipitation 2 ul, Immunohistochemistry-Paraffin 1:20 - 1:200, Immunohistochemistry-Frozen 1:20 - 1:200, Immunoblotting, Block/Neutralize

**Application Notes**

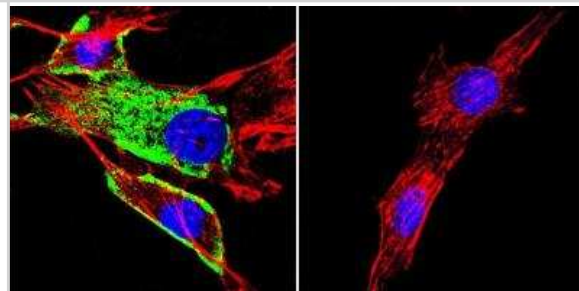
WB: Detects an approx. 70 kDa protein representing Hsc 70. By 2D gel electrophoresis, this antibody binds strongly to Hsc 70 and faintly to HSP 70 both before and after heat shock. IHC: Staining of Hsc 70 in mouse spermatids/spermatozoa results in staining restricted to the post acrosomal region in condensing spermatids and to the midpiece in spermatozoa. May be useful in IHC-Fr. Use in Immunoblotting reported in scientific literature (PMID 28095639). See [Simple Western Antibody Database](#) for Simple Western validation: Mouse Brain lysate as sample; separated by size; antibody dilution of 1:2000; matrix was 12-230 kDa; detected by Chemiluminescence.

**Images**

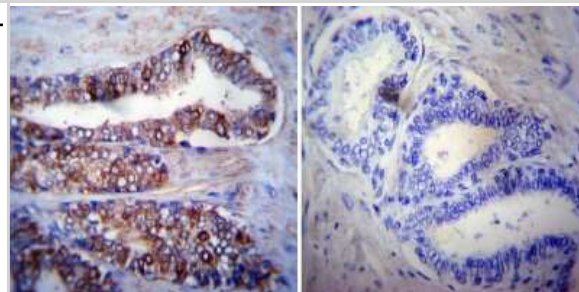
Western Blot: Hsp70 / Hsc70 Antibody (13D3) [NB120-2788] - Proteins were transferred to a PVDF membrane and blocked with 5% BSA/TBST for at least 1 hour. The membrane was probed with a HSP70 monoclonal antibody at a dilution of 1:1000 overnight at 4C on a rocking platform, washed in TBS-0.1%Tween 20, and probed with a goat anti-mouse IgM-HRP secondary antibody at a dilution of 1:20,000 for at least 1 hour.



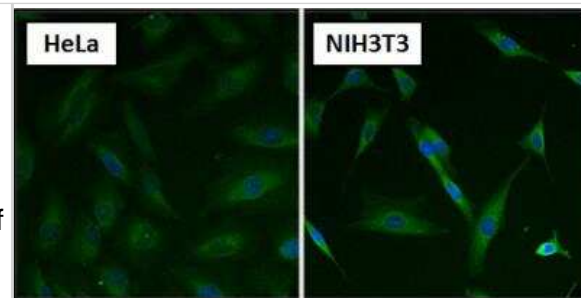
Immunocytochemistry/Immunofluorescence: Hsp70 / Hsc70 Antibody (13D3) [NB120-2788] - Analysis of HSC70 using Monoclonal antibody (13D3) shows staining in NIH-3T3 cells. HSC70 staining (green), F-Actin staining with Phalloidin (red) and nuclei with DAPI (blue) is shown. Cells were grown on chamber slides and fixed with formaldehyde prior to staining. Cells were probed without (control) or with or an antibody recognizing HSC70 at a dilution of 1:20-1:200 over night at 4C, washed with PBS and incubated with a DyLight-488 conjugated.



Immunohistochemistry-Paraffin: Hsp70 / Hsc70 Antibody (13D3) [NB120-2788] - Both normal and cancer biopsies of deparaffinized human Prostate carcinoma tissue.



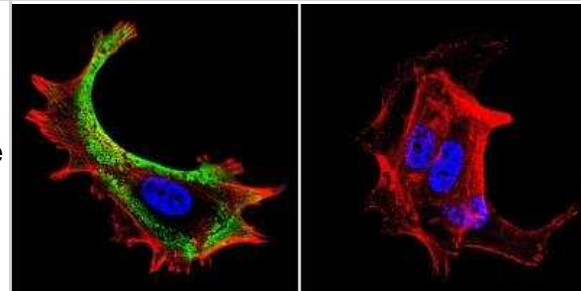
Immunocytochemistry/Immunofluorescence: Hsp70 / Hsc70 Antibody (13D3) [NB120-2788] - Formalin fixed cells were permeabilized with 0.1% Triton X-100 in TBS for 10 minutes at room temperature and blocked with 1% Blocker BSA for 15 minutes at room temperature. Cells were probed with a HSP70 monoclonal antibody at a dilution of 1:50 for at least 1 hour at room temperature, washed with PBS, and incubated with DyLight 488 goat anti-mouse IgG secondary antibody at a dilution of 1:400 for 30 minutes at room temperature. Nuclei (blue) were stained with Hoechst 33342 dye.



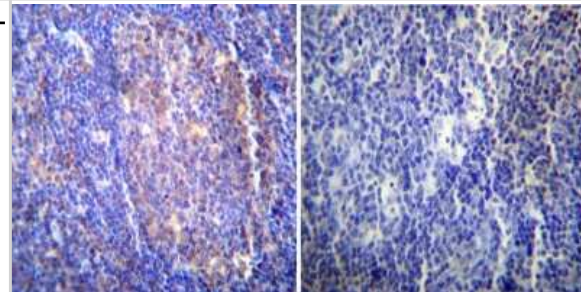
Immunocytochemistry/Immunofluorescence: Hsp70 / Hsc70 Antibody (13D3) [NB120-2788] - Analysis of HSC70 using HSC70 Monoclonal antibody (13D3) shows staining in HeLa cells. HSC70 staining (green), F-Actin staining with Phalloidin (red) and nuclei with DAPI (blue) is shown. Cells were grown on chamber slides and fixed with formaldehyde prior to staining. Cells were probed without (control) or with or an antibody recognizing HSC70 at a dilution of 1:20-1:200 over night at 4C, washed with PBS and incubated with a DyLight-488 conjugated.



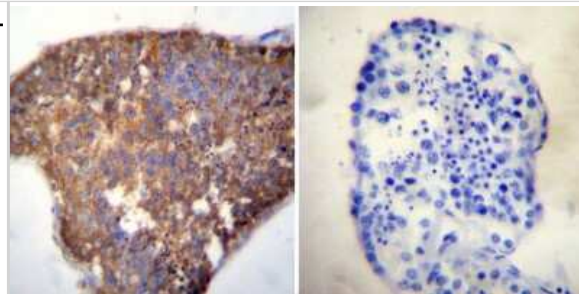
Immunocytochemistry/Immunofluorescence: Hsp70 / Hsc70 Antibody (13D3) [NB120-2788] - Analysis of HSC70 using HSC70 Monoclonal antibody (13D3) shows staining in MCF-7 cells. HSC70 staining (green), F-Actin staining with Phalloidin (red) and nuclei with DAPI (blue) is shown. Cells were grown on chamber slides and fixed with formaldehyde prior to staining. Cells were probed without (control) or with or an antibody recognizing HSC70 at a dilution of 1:20-1:200 C, washed with PBS and incubated with a DyLight-488 conjugated.



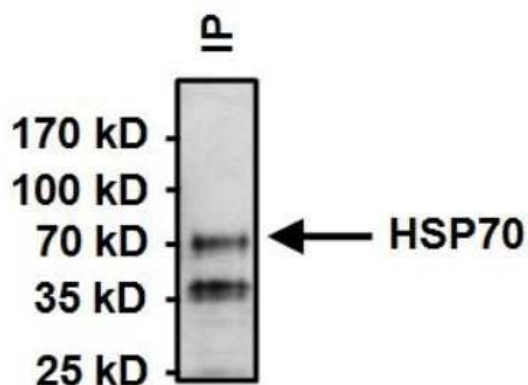
Immunohistochemistry-Paraffin: Hsp70 / Hsc70 Antibody (13D3) [NB120-2788] - Both normal and cancer biopsies of deparaffinized human Tonsil tissue.



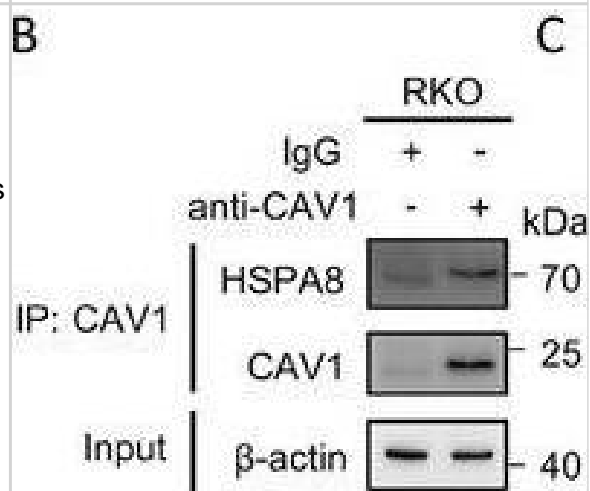
Immunohistochemistry-Paraffin: Hsp70 / Hsc70 Antibody (13D3) [NB120-2788] - Both normal and cancer biopsies of deparaffinized human Testis tissue.



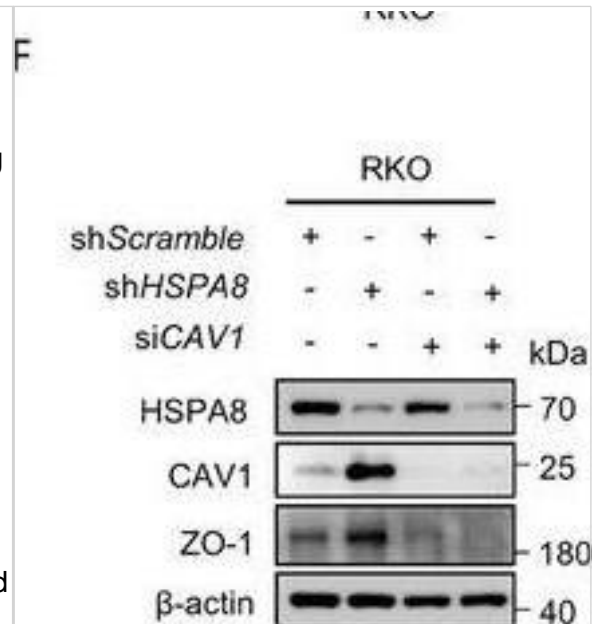
Immunoprecipitation: Hsp70 / Hsc70 Antibody (13D3) [NB120-2788] - Analysis of HSC70 was performed on HeLa cells. Antigen-antibody complexes were formed by incubating 500ug whole cell lysate with 2ul of HSC70 monoclonal antibody overnight on a rocking platform at 4C. The immune complexes were captured on 50ul Protein A/G Plus Agarose, washed extensively, and eluted with Lane Marker Reducing Sample Buffer. Samples were resolved on a 4-20% Tris-HCl polyacrylamide gel, transferred to a PVDF membrane, and blocked with 5% BSA/TBST for at least 1 hour. The membrane was probed with a HSC70 monoclonal antibody at a dilution of 1:1000 overnight rotating at 4C, washed in TBST, and probed with goat anti-mouse IgM-HRP secondary antibody for at least 1 hour. Chemiluminescent detection was performed using SuperSignal West Dura.



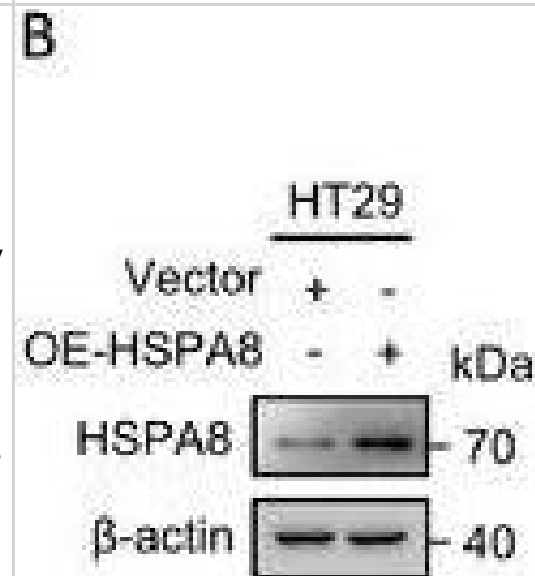
HSPA8 interacts with CAV1 through the KIFSN motif. A,B) The interaction between HSPA8 and CAV1 in RKO cells was determined by co-IP assays. C,D) The interaction between myc-HSPA8 and HA-CAV1 in HEK293T cells was determined by co-IP assays. E) KFERQ-like motifs within the protein sequence of CAV1 were identified using KFERQ finder software v0.8. F) Molecular docking of 3D structures predicts the binding of the CAV1 KIFSN motif (yellow) with HSPA8. G) A schematic representation of HA-CAV1 with full length (WT) and KIFSN motif deletion (Del). H,I) The interaction between myc-HSPA8 and HA-CAV1 (WT or Del) in HEK293T cells was determined by co-IP assays. J) The interaction between HSPA8 and HA-CAV1 with the S168A or S168D mutation in HEK293T cells was determined by co-IP assays. K) Potential kinases to phosphorylate the CAV1 S168 site predicted by NetPhos 3.1. L) The interaction between HA-CAV1 and p38 in HEK293T cells transfected with siNC or siMAPK14 was determined by co-IP assays. Image collected and cropped by CiteAb from the following open publication (<https://pubmed.ncbi.nlm.nih.gov/37973552>), licensed under a CC-BY license. Not internally tested by Novus Biologicals.



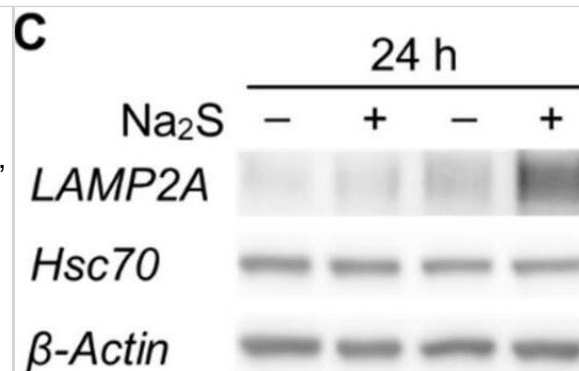
HSPA8 activates EMT by abrogating CAV1-mediated inhibition of the  $\beta$ -catenin/Wnt pathway in BRAF V600E CRC cells. A) The interactions between CAV1 and several proteins, including LAMP2A,  $\beta$ -catenin, and LC3, in HEK293T cells were determined by co-IP assays. B) The interaction between CAV1 and  $\beta$ -catenin in RKO cells stably expressing shScramble or shHSPA8 was determined by co-IP assays. C) Immunoblotting analysis of  $\beta$ -catenin protein expression in the cytoplasm or nucleus in RKO cells stably expressing shScramble or shHSPA8. GAPDH is used as cytoplasmic marker and Histone 3 (H3) is a nuclear marker. D,E) Immunofluorescence assays display the subcellular localization of  $\beta$ -catenin in RKO cells transfected with shScramble, shHSPA8, shScramble+siCAV1, or shHSPA8+siCAV1. Scale bar: 10  $\mu$ m. F) Immunoblotting analysis of the expression of HSPA8, CAV1, and ZO-1 in RKO cells transfected with shScramble, shHSPA8, shScramble+siCAV1, or shHSPA8+siCAV1. G,H) Transwell assays showing the cell migration and invasion of RKO cells transfected with shScramble, shHSPA8, or shHSPA8+siCAV1. Scale bar: 100  $\mu$ m. I,J) Wound healing assay showing the migration of RKO cells transfected with shScramble, shHSPA8, or shHSPA8+siCAV1 after 24 h. Scale bar: 200  $\mu$ m. K) Real-time qPCR analysis was performed to examine the mRNA expression levels (mean  $\pm$  SEM) of MMPs in RKO cells stably expressing shScramble or shHSPA8. \*\*\* $P < 0.001$ , \*\* $P < 0.01$ , \* $P < 0.05$ , and data are the mean  $\pm$  SEM from at least three independent experiments. Image collected and cropped by CiteAb from the following open publication (<https://pubmed.ncbi.nlm.nih.gov/37973552>), licensed under a CC-BY license. Not internally tested by Novus Biologicals.



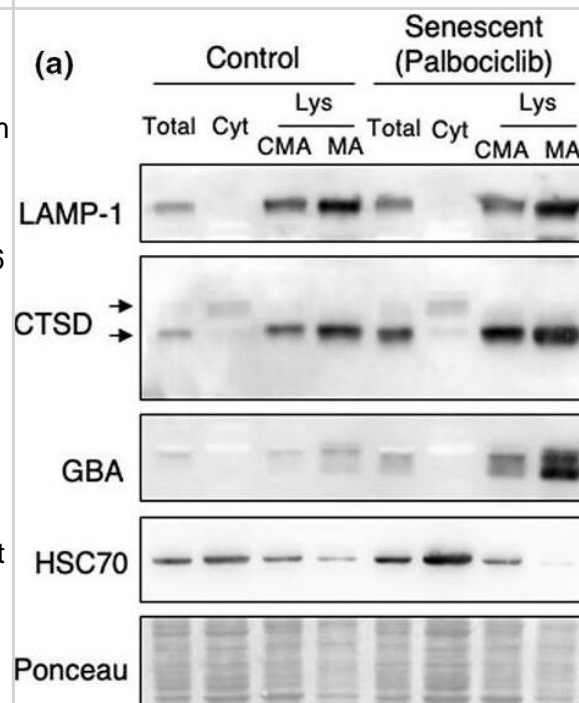
HSPA8 promotes epithelial-mesenchymal transition in BRAF V600E CRC cells. A) Immunoblotting analysis of RKO cells stably expressing shScramble, shHSPA8, or shHSPA8+OE-HSPA8. B) Immunoblotting analysis of HT29 cells stably expressing vector or HSPA8. C,D) Immunoblotting analysis of the effects of HSPA8 on the expression of EMT marker proteins in RKO and HT29 cells. E-H) Transwell assay showing the migration and invasion ability of RKO cells transfected with shScramble, shHSPA8, or shHSPA8+OE-HSPA8 and HT29 cells stably expressing vector or HSPA8. Scale bar: 100  $\mu$ m. I-L) Wound healing assay showing the migration of RKO cells transfected with shScramble, shHSPA8, or shHSPA8+OE-HSPA8 and HT29 cells stably expressing vector or HSPA8 after 24 h. Scale bar: 200  $\mu$ m. M-P) Transwell assays showing the effects of HSPA8 and Dabrafenib/Encorafenib on cell migration and invasion. Scale bar: 100  $\mu$ m. Q-S) Representative images of the colony formation of the indicated cells and quantification of clone numbers. \*\*\* $P < 0.001$ , \*\* $P < 0.01$ , \* $P < 0.05$ , and data are the mean  $\pm$  SEM from at least three independent experiments. Image collected and cropped by CiteAb from the following open publication (<https://pubmed.ncbi.nlm.nih.gov/37973552>), licensed under a CC-BY license. Not internally tested by Novus Biologicals.



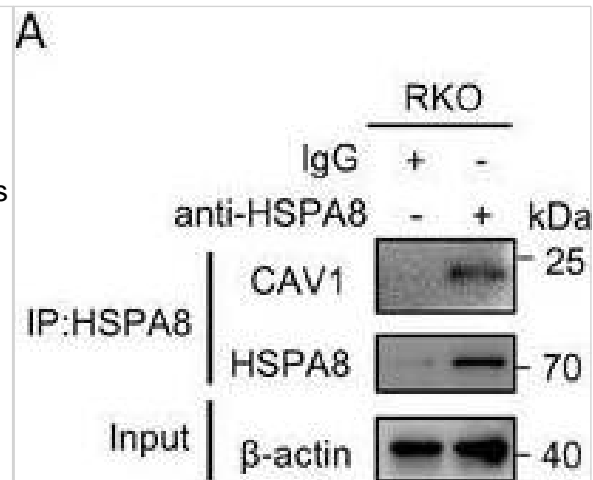
Effect of Na<sub>2</sub>S on the amounts of Nrf2 and CMA-related proteins in AD293 cells. (A) Immunoblot analyses of Nrf2 and  $\beta$ -actin in cell lysates from AD293 cells treated with Na<sub>2</sub>S (10  $\mu$ M) for 4 and 24 h. (B) Quantitative analyses of Nrf2 amounts from the immunoblot results shown in A. (C) Immunoblot analyses of CMA-related proteins (LAMP2A, Hsc70) and  $\beta$ -actin in cell lysates from AD293 cells treated with Na<sub>2</sub>S (10  $\mu$ M) for 24 h. (D) Quantitative analyses of LAMP2A and Hsc70 amounts from the immunoblot results shown in C. (E) Immunoblot analyses of a CMA/MA substrate (MEF2D) and  $\beta$ -actin in cell lysates from AD293 cells treated with Na<sub>2</sub>S (10  $\mu$ M) for 24 h. (F) Quantitative analysis of MEF2D amount from the immunoblot results shown in F. Whole blot images are presented in Figure S5. Amounts of  $\beta$ -actin were used as internal controls for quantification. Numbers in the columns represent the number of samples. \*  $p < 0.05$ , \*\*\*  $p < 0.001$  (unpaired t-test). Image collected and cropped by CiteAb from the following open publication (<https://pubmed.ncbi.nlm.nih.gov/35406792>), licensed under a CC-BY license. Not internally tested by Novus Biologicals.



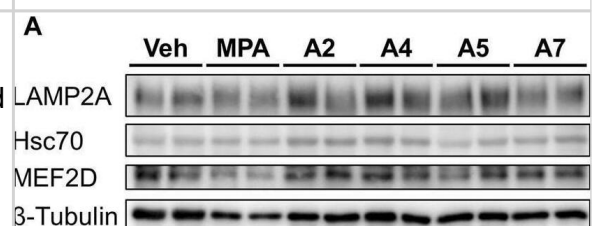
Lysosomal isolation and mass spectrometry analysis of constitutive resident proteins. (a) Western blot analysis for LAMP1, LAMP2A, CTSD, GBA, and HSC70 in homogenate (Total), cytosol (Cyt), and lysosomes (Lys) with high CMA activity (CMA) or high MA activity (MA) isolated from control or palbociclib-treated SK-MEL-103 cells. Arrows indicate precursor and mature form. Ponceau staining is shown as loading control. (b) Scheme of the hypothetical changes in levels of proteins in lysosomes treated or not with ammonium chloride and leupeptin (N/L) 16 h before isolation. Proteins are classified depending on these changes as degraded (lysosomal substrates) if they accumulate upon N/L treatment, or constitutive (resident proteins) if they do not accumulate upon N/L treatment. (c) Principal component analysis (PCA) of the CMA and MA lysosome samples,  $n = 3$  with two technical replicates each. (d) Changes in abundance of the lysosomal constitutive proteins in CMA and MA lysosomes. Constitutive proteins were defined as those that do not change significantly  $p > 0.05$  in N/L versus vehicle or that have a negative log<sub>2</sub> fold change N/L versus vehicle. (e) Top lysosomal resident proteins found at higher or lower levels in CMA and MA lysosomes. (f) Fold change (over control) in protein levels of TOR protein components found in both CMA and MA lysosomes. Image collected and cropped by CiteAb from the following open publication (<https://pubmed.ncbi.nlm.nih.gov/36087066>), licensed under a CC-BY license. Not internally tested by Novus Biologicals.



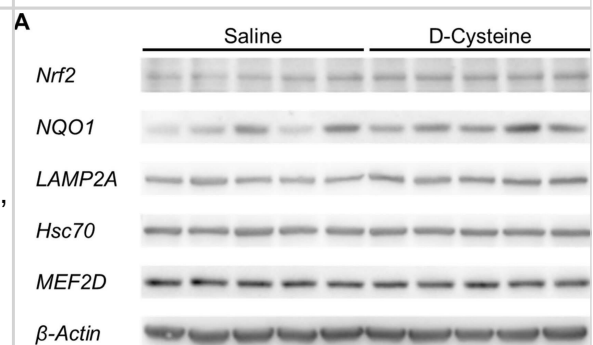
HSPA8 interacts with CAV1 through the KIFSN motif. A,B) The interaction between HSPA8 and CAV1 in RKO cells was determined by co-IP assays. C,D) The interaction between myc-HSPA8 and HA-CAV1 in HEK293T cells was determined by co-IP assays. E) KFERQ-like motifs within the protein sequence of CAV1 were identified using KFERQ finder software v0.8. F) Molecular docking of 3D structures predicts the binding of the CAV1 KIFSN motif (yellow) with HSPA8. G) A schematic representation of HA-CAV1 with full length (WT) and KIFSN motif deletion (Del). H,I) The interaction between myc-HSPA8 and HA-CAV1 (WT or Del) in HEK293T cells was determined by co-IP assays. J) The interaction between HSPA8 and HA-CAV1 with the S168A or S168D mutation in HEK293T cells was determined by co-IP assays. K) Potential kinases to phosphorylate the CAV1 S168 site predicted by NetPhos 3.1. L) The interaction between HA-CAV1 and p38 in HEK293T cells transfected with siNC or siMAPK14 was determined by co-IP assays. Image collected and cropped by CiteAb from the following open publication (<https://pubmed.ncbi.nlm.nih.gov/37973552>), licensed under a CC-BY license. Not internally tested by Novus Biologicals.



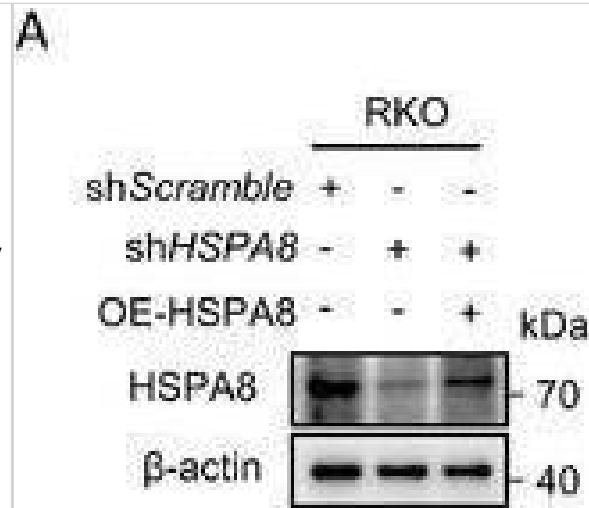
Effects of ar-turmerone analogs on the expression of CMA-related proteins and mRNAs in SH-SY5Y cells stably expressing GAPDH-HT. (A) Representative immunoblot images of LAMP2A, Hsc70, MEF2D, and β-tubulin in cells treated with vehicle, 5 μM MPA, or ar-turmerone analogs (20 μM) for 24 h. (B) Quantitative analyses of the immunoreactive bands of LAMP2A, Hsc70, and MEF2D. The band intensities were normalized with the bands of β-tubulin as an internal control. Data are presented as the mean ± SEM of four different samples. \*p < 0.05, \*\*p < 0.01, \*\*\*p < 0.001 vs. vehicle (one-way ANOVA, followed by a post hoc Tukey test). (C) The mRNA amounts of LAMP2A, LAMP2B, LAMP1, HSPA8 (Hsc70), TFEB, and MEF2D were quantified with RT-qPCR. Cells were treated with vehicle, 20 μM A2, or 20 μM A4 for 24 h. The data are presented as the mean ± SEM of four independent samples. \*p < 0.05, \*\*p < 0.01, \*\*\*p < 0.001 vs. vehicle (one-way ANOVA, followed by a post hoc Tukey test). Image collected and cropped by CiteAb from the following open publication (<https://www.frontiersin.org/articles/10.3389/fcell.2024.1418296/full>), licensed under a CC-BY license. Not internally tested by Novus Biologicals.



Effect of long-term treatment with D-cysteine on the amounts of Nrf2- and CMA-related proteins in cerebellar lysates from ICR mice. (A) Immunoblot analyses of Nrf2, NQO1, LAMP2A, Hsc70, MEF2D, and β-actin in cerebellar lysates from ICR mice daily treated with saline (Sal) and D-cysteine (100 mg/kg/day) for 10 weeks. Whole blot images are presented in Figure S6. (B) Quantitative analyses of the amounts of Nrf2, NQO1, LAMP2A, Hsc70, and MEF2D shown in A. Amounts of β-actin were used as internal controls for the quantification. \* p < 0.05, \*\* p < 0.01 vs. saline-treated mice (unpaired t-test, n = 5 in both saline- and D-cysteine-treated mice). Image collected and cropped by CiteAb from the following open publication (<https://pubmed.ncbi.nlm.nih.gov/35406792>), licensed under a CC-BY license. Not internally tested by Novus Biologicals.



HSPA8 promotes epithelial-mesenchymal transition in BRAF V600E CRC cells. A) Immunoblotting analysis of RKO cells stably expressing shScramble, shHSPA8, or shHSPA8+OE-HSPA8. B) Immunoblotting analysis of HT29 cells stably expressing vector or HSPA8. C,D) Immunoblotting analysis of the effects of HSPA8 on the expression of EMT marker proteins in RKO and HT29 cells. E-H) Transwell assay showing the migration and invasion ability of RKO cells transfected with shScramble, shHSPA8, or shHSPA8+OE-HSPA8 and HT29 cells stably expressing vector or HSPA8. Scale bar: 100  $\mu$ m. I-L) Wound healing assay showing the migration of RKO cells transfected with shScramble, shHSPA8, or shHSPA8+OE-HSPA8 and HT29 cells stably expressing vector or HSPA8 after 24 h. Scale bar: 200  $\mu$ m. M-P) Transwell assays showing the effects of HSPA8 and Dabrafenib/Encorafenib on cell migration and invasion. Scale bar: 100  $\mu$ m. Q-S) Representative images of the colony formation of the indicated cells and quantification of clone numbers. \*\*\* $P < 0.001$ , \*\* $P < 0.01$ , \* $P < 0.05$ , and data are the mean  $\pm$  SEM from at least three independent experiments. Image collected and cropped by CiteAb from the following open publication (<https://pubmed.ncbi.nlm.nih.gov/37973552>), licensed under a CC-BY license. Not internally tested by Novus Biologicals.



## Publications

Zhang Y, Wu H, Zhang Q et al. LAMP2A-mediated neuronal hyperexcitability by enhancing NKA $\beta$ 1 degradation underlies depression-induced allodynia. *Cell reports* 2025-04-02 [PMID: 40178973]

Maestri A, Ehrenborg E, Werngren O et al. Titration-WB: A methodology for accurate quantitative protein determination overcoming reproducibility errors. *PLoS ONE* 2025-06-12 [PMID: 40504814]

Choi YJ, Yun SH, Yu J et al. Chaperone-mediated autophagy dysregulation during aging impairs hepatic fatty acid oxidation via accumulation of NCoR1 *Molecular metabolism* 2023-07-29 [PMID: 37524243] (Western Blot)

M Rovira, R Sereda, D Pladevall-, V Ramponi, I Marin, M Maus, J Madrigal-M, A Díaz, F García, J Muñoz, AM Cuervo, M Serrano The lysosomal proteome of senescent cells contributes to the senescence secretome *Aging Cell*, 2022-09-10;0(0):e13707. 2022-09-10 [PMID: 36087066] (Western Blot)

Bourdenx M, Martín-Segura A, Scrivo A et al. Chaperone-mediated autophagy prevents collapse of the neuronal metastable proteome *Cell* 2021-05-01 [PMID: 33891876] (Western Blot)

Li B, Ming H, Qin S et al. HSPA8 Activates Wnt/ $\beta$ -Catenin Signaling to Facilitate BRAF V600E Colorectal Cancer Progression by CMA-Mediated CAV1 Degradation *Advanced science* (Weinheim, Baden-Wurttemberg, Germany) 2023-11-16 [PMID: 37973552]

Krause, GJ;Kirchner, P;Stiller, B;Morozova, K;Diaz, A;Chen, KH;Krogan, NJ;Agullo-Pascual, E;Clement, CC;Lindenau, K;Swaney, DL;Dilipkumar, S;Bravo-Cordero, JJ;Santambrogio, L;Cuervo, AM; Molecular determinants of the crosstalk between endosomal microautophagy and chaperone-mediated autophagy *Cell reports* 2023-12-05 [PMID: 38060380]

Mario Fernández Comaduran, Sandra Minotti, Suleima Jacob-Tomas, Javeria Rizwan, Nancy Larochelle, Richard Robitaille, Chantelle F. Sephton, Maria Vera, Josephine N. Nalbantoglu, Heather D. Durham Impact of histone deacetylase inhibition and arimoclomol on heat shock protein expression and disease biomarkers in primary culture models of familial ALS *Cell Stress & Chaperones* 2024-04-01 [PMID: 38570009]

Li J, Yao H, Zhao F et al. Pycard deficiency inhibits microRNA maturation and prevents neointima formation by promoting chaperone-mediated autophagic degradation of AGO2/argonaute 2 in adipose tissue *Autophagy* 2023-11-14 [PMID: 37963060] (IHC-P, IP, Mouse)

### Details:

IHC-P Dilution 1:300; IP Dilution: 1 $\mu$ g of antibody was added to 500 $\mu$ g of cell lysate and incubated overnight at 4°C, and then incubated with protein A agarose beads for 4h

Idera, A;Sharkey, LM;Kurauchi, Y;Kadoyama, K;Paulson, HL;Katsuki, H;Seki, T; Wild-type and pathogenic forms of ubiquilin 2 differentially modulate components of the autophagy-lysosome pathways *Journal of pharmacological sciences* 2023-07-01 [PMID: 37257946] (Western Blot, Human)

Ueda E, Ohta T, Konno A et al. D-Cysteine Activates Chaperone-Mediated Autophagy in Cerebellar Purkinje Cells via the Generation of Hydrogen Sulfide and Nrf2 Activation *Cells* 2022-04-05 [PMID: 35406792] (WB)

Wang D, Tan KS, Zeng W et al. Hepatocellular BChE as a therapeutic target to ameliorate hypercholesterolemia through PRMT5 selective degradation to restore LDL receptor transcription *Life sciences* 2022-01-19 [PMID: 35065166]

More publications at <http://www.novusbio.com/NB120-2788>





### **Novus Biologicals USA**

10730 E. Briarwood Avenue  
Centennial, CO 80112  
USA  
Phone: 303.730.1950  
Toll Free: 1.888.506.6887  
Fax: 303.730.1966  
nb-customerservice@bio-techne.com

### **Bio-Techne Canada**

21 Canmotor Ave  
Toronto, ON M8Z 4E6  
Canada  
Phone: 905.827.6400  
Toll Free: 855.668.8722  
Fax: 905.827.6402  
canada.inquires@bio-techne.com

### **Bio-Techne Ltd**

19 Barton Lane  
Abingdon Science Park  
Abingdon, OX14 3NB, United Kingdom  
Phone: (44) (0) 1235 529449  
Free Phone: 0800 37 34 15  
Fax: (44) (0) 1235 533420  
info.EMEA@bio-techne.com

### **General Contact Information**

www.novusbio.com  
Technical Support: nb-technical@bio-techne.com  
Orders: nb-customerservice@bio-techne.com  
General: novus@novusbio.com

### **Products Related to NB120-2788**

---

NBP2-33376H	Blue Marker Antibody (6F4-F6) [HRP]
HAF007	Goat anti-Mouse IgG Secondary Antibody [HRP]
NB7539	Goat anti-Mouse IgG (H+L) Secondary Antibody [HRP]
NBP1-97007	Mouse IgM Isotype Control

---

### **Limitations**

This product is for research use only and is not approved for use in humans or in clinical diagnosis. Primary Antibodies are guaranteed for 1 year from date of receipt.

For more information on our 100% guarantee, please visit [www.novusbio.com/guarantee](http://www.novusbio.com/guarantee)

Earn gift cards/discounts by submitting a review: [www.novusbio.com/reviews/submit/NB120-2788](http://www.novusbio.com/reviews/submit/NB120-2788)

Earn gift cards/discounts by submitting a publication using this product:  
[www.novusbio.com/publications](http://www.novusbio.com/publications)

